Published June 1, 2009

The *S. pombe* mitotic regulator Cut12 promotes spindle pole body activation and integration into the nuclear envelope

Victor A. Tallada,[1] Kenji Tanaka,[2] Mitsuhiro Yanagida,[3] and Iain M. Hagan[1,3]

[1]Cancer Research UK Cell Division Group, Paterson Institute for Cancer Research, University of Manchester, Manchester M20 4BX, England, UK
[2]Research Institute for Disease Mechanism and Control, Nagoya University School of Medicine, Showa-ku, Nagoya 466-8550, Japan
[3]Graduate School of Biostudies, Kyoto University, Sakyo-ku, Kyoto 606-8501, Japan

The fission yeast spindle pole body (SPB) comprises a cytoplasmic structure that is separated from an ill-defined nuclear component by the nuclear envelope. Upon mitotic commitment, the nuclear envelope separating these domains disperses as the two SPBs integrate into a hole that forms in the nuclear envelope. The SPB component Cut12 is linked to cell cycle control, as dominant *cut12.s11* mutations suppress the mitotic commitment defect of *cdc25.22* cells and elevated Cdc25 levels suppress the monopolar spindle phenotype of *cut12.1* loss of function mutations. We show that the *cut12.1* monopolar phenotype arises from a failure to activate and integrate the new SPB into the nuclear envelope. The activation of the old SPB was frequently delayed, and its integration into the nuclear envelope was defective, resulting in leakage of the nucleoplasm into the cytoplasm through large gaps in the nuclear envelope. We propose that these activation/integration defects arise from a local deficiency in mitosis-promoting factor activation at the new SPB.

Introduction

The dynamic properties of the microtubule cytoskeleton underpin a range of cellular functions from cell migration to division. In a large number of eukaryotes, the challenge of generating a malleable and dynamic yet tightly regulated array is facilitated by restraining microtubule nucleation to discrete sites called microtubule-organizing centers (MTOCs). This localized microtubule nucleation from MTOCs can then be tightly controlled by regulating MTOC number and activity to modulate the architecture of the microtubule cytoskeleton. Therefore, understanding MTOC composition and control is central to the understanding of a spectrum of cell functions. The genetic tractability or lifestyle of several microbial systems has meant that many of the core principles of MTOC composition function have been established by the analysis of microbial model systems such as *Chlamydomonas reinhardtii*, *Aspergillus nidulans*, *Tetrahymena thermophila*, *Saccharomyces cerevisiae*, and the subject of this study, the fission yeast *Schizosaccharomyces pombe* (Oakley and Oakley, 1989; Hagan and Petersen, 2000; Dutcher, 2003; Jaspersen and Winey, 2004; Kilburn et al., 2007).

Mitotic commitment in *S. pombe* is accompanied by a dramatic change in the microtubule cytoskeleton, as cytoplasmic microtubules depolymerize and microtubules are nucleated by the two spindle pole bodies (SPBs; McCully and Robinow, 1971; Hagan and Hyams, 1988; Ding et al., 1993, 1997). The SPB is composed of a large cytoplasmic component that is connected to a poorly defined nuclear component by fine striations that run through the nuclear envelope that separates these two domains (Ding et al., 1997). SPB duplication in fission yeast is poorly understood. Genetic analyses and a recent EM study suggest that duplication occurred in G1 phase of the cell cycle (Vardy and Toda, 2000; Uzawa et al., 2004), whereas another EM study suggested that it was in G2 phase (Ding et al., 1997). The clear presence of a bridge structure between the cytoplasmic components of duplicated SPBs suggests that duplication in

Correspondence to Iain M. Hagan: ihagan@picr.man.ac.uk

V.A. Tallada's present address is Centro Andaluz de Biología del Desarrollo, Universidad Pablo de Olavide/Consejo Superior de Investigaciones Cientificas, 41013 Sevilla, Spain.

K. Tanaka's present address is National Institute of Technology and Evaluation, Kisarazu-shi, Chiba 292-0818, Japan.

Abbreviations used in this paper: β-Gal, β-galactosidase; MPF, mitosis-promoting factor; MTOC, microtubule-organizing center; SPB, spindle pole body.

Supplemental Material can be found at:
http://jcb.rupress.org/content/suppl/2009/06/01/jcb.200812108.DC1.html

The Rockefeller University Press $30.00
J. Cell Biol. Vol. 185 No. 5 875–888
www.jcb.org/cgi/doi/10.1083/jcb.200812108

Published June 1, 2009

fission yeast may well mimic that in budding yeast SPB, in which a half bridge extends from one side of the SPB to form a full bridge that is capped by a satellite structure from which a new SPB is assembled (McCully and Robinow, 1971; Ding et al., 1997; Adams and Kilmartin, 2000). Such conservative duplication is consistent with the ability to differentiate between old and new SPBs with a slow folding fluorescent protein in both budding and fission yeast (Pereira et al., 2001; Grallert et al., 2004).

The nuclear envelope that separates the nuclear and cytoplasmic components fragments upon commitment to mitosis to generate a fenestra in the nuclear membrane (Ding et al., 1997). This localized nuclear envelope breakdown is confined to the region within the SPBs. The two SPB domains then fuse to plug this hole and nucleate microtubules to form the spindle. During anaphase B, the nuclear envelope grows back once more between the two components to completely separate them in the next cycle (Ding et al., 1997).

The SPB components Cut11 and Sad1 contain regions that have the potential to integrate into the nuclear membrane (Hagan and Yanagida, 1995; West et al., 1998). Cut11 is the fission yeast equivalent of the conserved Ndc1 protein that was first identified because it was required for the insertion of the budding yeast SPB into the nuclear envelope (Winey et al., 1993; West et al., 1998; Stavru et al., 2006). Metazoan Ndc1 associates with nuclear pores throughout interphase, whereas budding yeast Ndc1 associates with both the SPBs and nuclear pores throughout the cell cycle (Chial et al., 1998; Stavru et al., 2006). Like other Ndc1 family members, *cut11*$^{+}$ encodes six or seven regions that are predicted to constitute membrane-spanning domains (West et al., 1998; Stavru et al., 2006), and it associates with nuclear pores throughout the cell cycle and the SPB in mitosis. EM of a temperature-sensitive *cut11* mutant revealed monopolar spindles emanating from a single SPB and a defect in SPB integration into the nuclear membrane. In extreme cases, SPBs failed to insert into the fenestra in the nuclear envelope and fell into the nucleoplasm (West et al., 1998). Sad1 possesses a single trans-membrane–spanning domain and is the founding member of the SUN (Sad1/UNC-84) domain family of proteins that anchors centrosomes to nuclear envelopes in higher eukaryotes (Hagan and Yanagida, 1995; Malone et al., 1999; Tzur et al., 2006; Wilhelmsen et al., 2006). In fission yeast, Sad1 has been linked to the association of centromeres with the interphase SPB (Funabiki et al., 1993; Goto et al., 2001; King et al., 2008).

The *cut12*$^{+}$ gene also encodes an SPB component (Bridge et al., 1998). Like the *cut11.1* mutant, *cut12.1* arrests mitotic commitment because it forms a monopolar rather than a bipolar spindle (Bridge et al., 1998; West et al., 1998). In the case of *cut12.1*, staining with antibodies to Sad1 has established that microtubules emanate from just one of the two SPBs and that Sad1 is often preferentially enriched on the nonfunctional SPB (Bridge et al., 1998). *cut12.1* and *cut11.1* mutants display synthetic lethality, suggesting that Cut12 may function in concert with Cut11 and so, potentially, may have a role in SPB insertion into the nuclear envelope (West et al., 1998). However, the cloning of *cut12*$^{+}$ showed that it does not contain any regions that would be predicted to span the nuclear envelope and led to the unexpected realization that *cut12*$^{+}$ was allelic to the *stf1*$^{+}$ gene (Bridge et al., 1998). The dominant *stf1* mutations had been identified as suppressors of conditional mutations in the Cdc25 phosphatase that remove the inhibitory phosphate from Cdc2 during mitotic commitment (Hudson et al., 1990, 1991). Further genetic analysis has revealed that enhancing Cdc25 levels suppresses the *cut12.1* mutation, and the *cdc25.22* mutation exacerbates the phenotype of *cut12.1* mutants (Bridge et al., 1998; Tallada et al., 2007). This reciprocal relationship between Cdc25 and Cut12 indicates that this SPB component plays a major role in regulating commitment to mitosis. Several studies indicate that this impact is likely to be exerted through alterations in the behavior of the mitosis-promoting factor (MPF), amplifying the positive feedback loop kinase polo with which it associates (Mulvihill et al., 1999; MacIver et al., 2003; Petersen and Hagan, 2005).

S. pombe polo kinase, Plo1, normally associates with mitotic and late G2 interphase SPBs (Bähler et al., 1998; Mulvihill et al., 1999). The *stf1.1* gain of function mutation of *cut12* (referred to from here on as *cut12.s11*) enhances the recruitment of Plo1 to the G2 SPB and boosts the activity of the kinase throughout the cell cycle (Mulvihill et al., 1999; MacIver et al., 2003). Furthermore, mutation of a single residue on Plo1 to glutamic acid to mimic phosphorylation also increases Plo1 recruitment to the G2 SPB and accelerates mitotic commitment (Petersen and Hagan, 2005; Petersen and Nurse, 2007). Crucially, mutation of this same residue to alanine stops both the suppression of *cdc25.22* and the interphase recruitment of Plo1 that is induced by the *cut12.s11* mutation. It also blocks the ability of constitutively active Plo1 to suppress *cdc25.22* (Petersen and Hagan, 2005). Thus, the recruitment of polo kinase to the SPB plays a key role in regulating commitment to mitosis in fission yeast and couples mitotic control to signaling from the nutrient-sensing TOR (target of rapamycin) kinase pathway and the fission yeast NIMA (never in mitosis A)-related kinase Fin1 (Grallert and Hagan, 2002; Petersen and Nurse, 2007).

In this study, we characterize the *cut12.1* phenotype at the level of EM and address the distinction between the functions of Cut12 in promoting the mitotic state of the SPB and Cut11 in physically inserting the SPB into the nuclear envelope. We show that the new SPB appears to be unable to be converted into a mitotic state and insert into the nuclear envelope in *cut12.1*. The old SPB is activated to nucleate microtubules; however, its integration into the nuclear envelope is defective, resulting in a gapped membrane deformation in the nuclear envelope through which nucleoplasm leaks into the cytoplasm. We discuss why we believe that this SPB insertion defect arises from defective MPF activation at the SPB.

Results

One SPB fails to insert into the nuclear envelope of *cut12.1* cells

We previously established that one of the two SPBs fails to nucleate microtubules when *cut12.1* cells are shifted from the permissive temperature of 25°C to the restrictive temperature of 36°C (Bridge et al., 1998). To understand this phenotype in greater detail, we processed *cut12.1* cells for EM analysis 100 min after

Published June 1, 2009

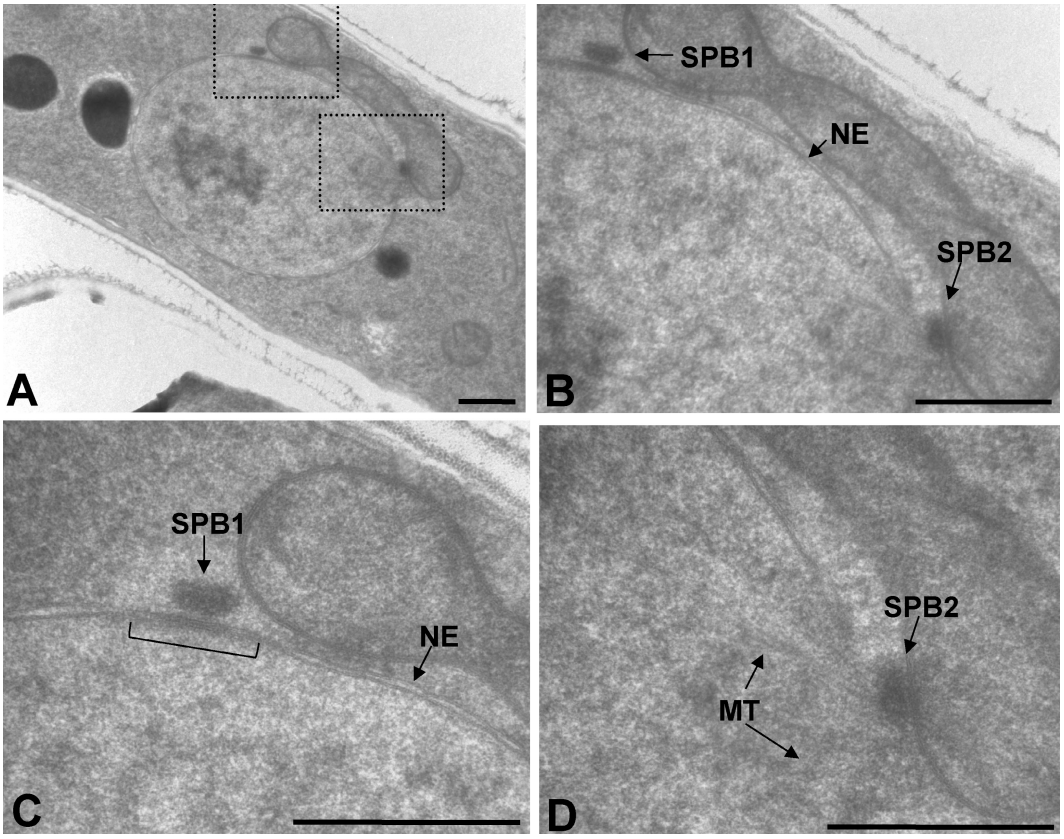

Figure 1. **One SPB fails to insert in *cut12.1* mutant cells at 36°C.** (A–D) *cut12.1* cells were grown to mid-log phase in minimal medium at 25°C and shifted to 36°C after synchronization by centrifugal elutriation. 100 min after the shift, when the condensed chromosome index was 30%, cells were fixed by high pressure freezing and processed for transmission EM. The panels show different magnifications of the same section of a mutant mitotic nucleus. The enlargements in C and D correspond to the regions delimited by the dotted boxes in A. Although the cell is clearly in mitosis because the right SPB (SPB2) is nucleating microtubules (MT, arrows), the left SPB (SPB1) has not inserted into the nuclear envelope (NE) and retains the region of differentiated nuclear envelope that is typical of interphase SPBs (indicated by the bracket in C), which presents an electron-dense material. Only the pole that is inserted is nucleating mitotic microtubules. It is noteworthy that the connection between the mitochondria and the SPB reported in previous EM analyses of mitotic cells is maintained in the defective mitoses of *cut12.1* cells (McCully and Robinow, 1971; Kanbe et al., 1989). Bars, 500 nm.

the temperature of a G2 culture had been shifted from the permissive temperature of 25°C to the restrictive temperature of 36°C. Analysis of serial sections through the nuclei of eight different cells established that, in every case, the inactive SPB failed to insert into the nuclear envelope when Cut12 function was compromised in this way (Fig. 1, SPB1; and Figs. S1 and S2). The structure of this inactive SPB was strikingly reminiscent of images of the interphase SPB of a wild-type cell (Ding et al., 1997), with a highly differentiated nuclear envelope underlying the large cytoplasmic structure. Given that the *cut12.1* mutation is a recessive, loss of function mutation (Bridge et al., 1998), we conclude that Cut12 function is required to promote the integration of one of the two SPBs into the nuclear envelope.

The old SPB is the active SPB in *cut12.1* and *cut11.1*

SPB duplication is conservative (Grallert et al., 2004), raising the possibility that the failure of one of the SPBs to function at 36°C could arise because of an inherent difference between the old and the new SPB. SPB age in both budding and fission yeast can be determined by following the fluorescence of a fusion between the red fluorescent protein DsRed and a core SPB component. As the RFP moiety takes several hours to fold, very few cells in a logarithmically growing culture have fluorescent SPBs; however, arresting cell cycle progression by nitrogen starvation to induce a G1 arrest provides sufficient time for the protein in the majority of the SPBs in the population to fold into an actively fluorescing state. The RFP moiety that is associated with SPBs that form after readdition of a nitrogen source to restore cell division does not generally have time to fold so that the old SPB fluoresces, whereas the new one does not (Pereira et al., 2001). In fission yeast, fusion of RFP to the pericentrin homologue Pcp1 (Flory et al., 2002) enables the differentiation of the old and new SPB (Grallert et al., 2004). We used this nitrogen starvation regimen to label the old SPBs in a *cut12.1 pcp1.RFP* strain before shifting the culture to 36°C. The inclusion of the *nmt81.atb2GFP* gene fusion in this strain enabled us to monitor microtubules. 3 h after shifting the cells to 36°C, the majority of the culture was processed for immunofluorescence microscopy and stained with antibodies against α-tubulin and Sad1 (Hagan and Yanagida, 1995). The remainder of the culture was observed by live cell microscopy at 36°C.

Immunofluorescence microscopy of *cut12.1* cells established that 89% ($n = 52$) of mitotic cells had monopolar spindles. In 70% of these monopolar spindles, microtubules emanated from one of two distinct Sad1 SPB signals, whereas in the remaining

Published June 1, 2009

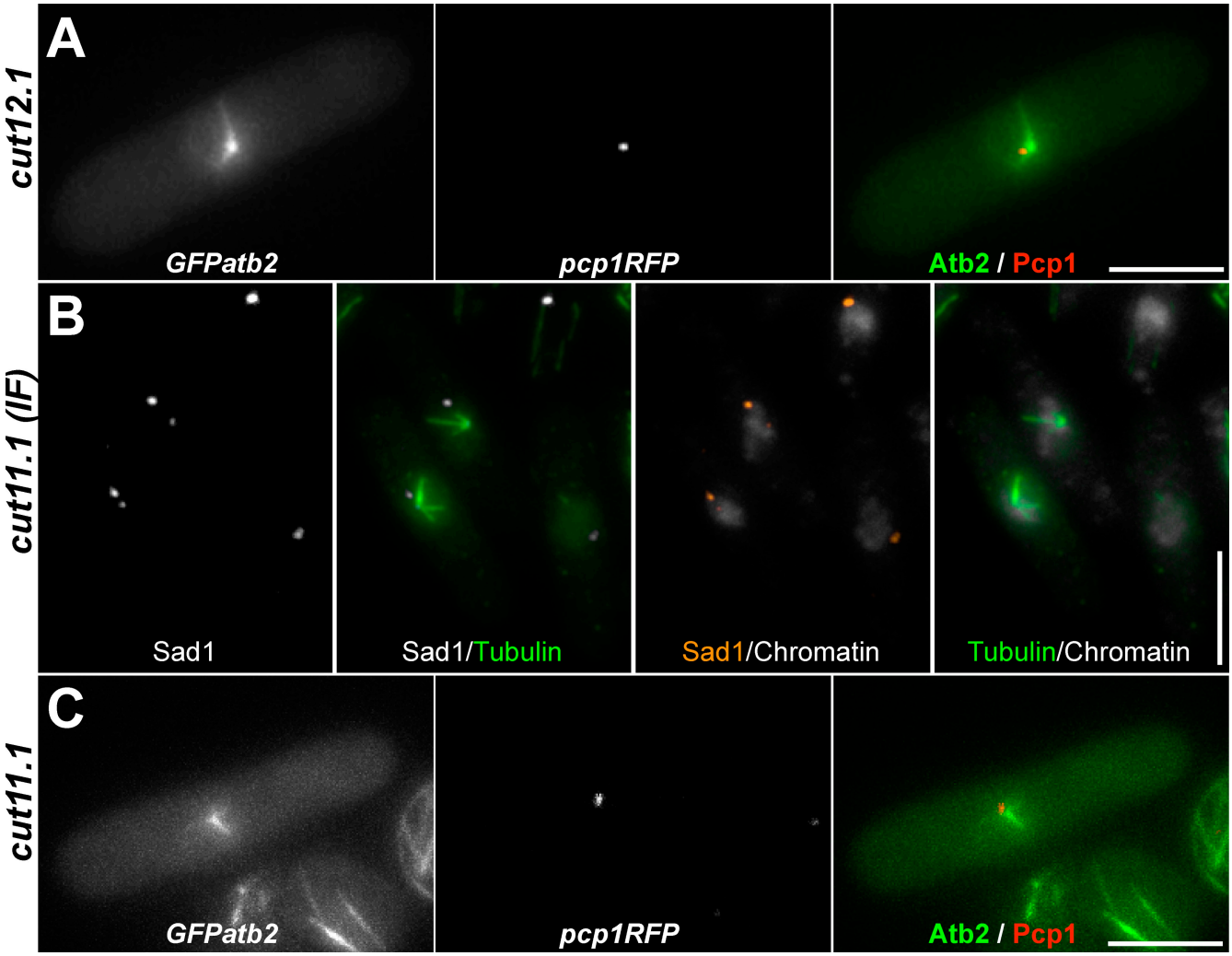

Figure 2. **The old pole nucleates microtubules in *cut12.1* and *cut11.1* defective mitoses.** (A–C) *cut12.1 pcp1.RFP nmt81.atb2GFP* (A) or *cut11.1 pcp1.RFP nmt81.atb2GFP* (B and C) cells were grown to mid-log phase at 25°C and starved by the removal of a nitrogen source for 14 h and 8 h, respectively, before being filtered and resuspended in nitrogen-containing minimal medium at a density of 1.5 × 10^6 cells/ml. 4 h after refeeding, both mutants were shifted to 36°C for 3 h, and samples were taken either for live cell imaging (A and C) or anti-Sad1/anti–α-tubulin immunofluorescence (IF) microscopy (B). In this case, DAPI was used to stain the chromatin. All combinations of two signals are shown using false colors. Although microtubules emerge from only one of two dots of Sad1 staining in *cut11.1* cells in B, microtubules emerge from the single (old SPB) staining in A and C. Note the asymmetry of Sad1 staining in *cut11.1* immunofluorescence (B, left). The more intense signal correlates with the nonactive SPB. Bars: (A and C) 5 µm; (B) 10 µm.

30%, the microtubules extended from a single focus of SPB staining (Bridge et al., 1998; unpublished data). In contrast, live cell imaging of the same population indicated that in all cells in which a single focus of SPB staining was discerned, the microtubules were extending from the RFP fluorescent marker on the old SPB (n = 21; Fig. 2 A). We conclude that it is the new SPB that fails to activate and insert into the nuclear envelope in *cut12.1* mutants.

Given the strong genetic interactions between *cut12.1* and *cut11.1* mutants (West et al., 1998), we asked whether there was a similar association between the competence of the SPB to nucleate microtubules and SPB age in *cut11.1* mutants. Sad1/tubulin immunofluorescence analysis of the *cut11.1 nmt81.GFPatb2 pcp1.RFP* cultures used for live cell analysis established that 65.5% (n = 61) of the cells with monopolar spindles had two clear Sad1 foci, with the microtubule nucleating SPB often recruiting less Sad1 than the inactive one (Fig. 2 B). The monopolar GFP tubulin signal in live cell imaging of the same culture emanated from a single red fluorescent Pcp1.RFP signal in all 17 cells examined (Fig. 2 C). We conclude that it is the new SPB of both *cut12.1* and *cut11.1* mutant cells that fails to insert into the nuclear envelope at 36°C (West et al., 1998).

Nuclear/cytoplasmic partitioning persists in wild-type mitosis

In addition to the SPB activation defect addressed in the previous sections, EM analysis revealed gapped membrane distortions in the nuclear envelope of *cut12.1* cells at 36°C (Fig. 3, A–D). In many instances, the nucleoplasm spilled out through this gapped membrane distortion to mix with the cytoplasm (Fig. 3, A and D). When SPBs were discerned in a section with a hole in the nuclear envelope, the SPB was always adjacent to the hole (Fig. 3, A–C). Although we failed to observe such holes in or any distortion of the nuclear envelopes of wild-type cells (unpublished data), it is possible that the *cut12.1* mutant cells had intact nuclear envelopes

Published June 1, 2009

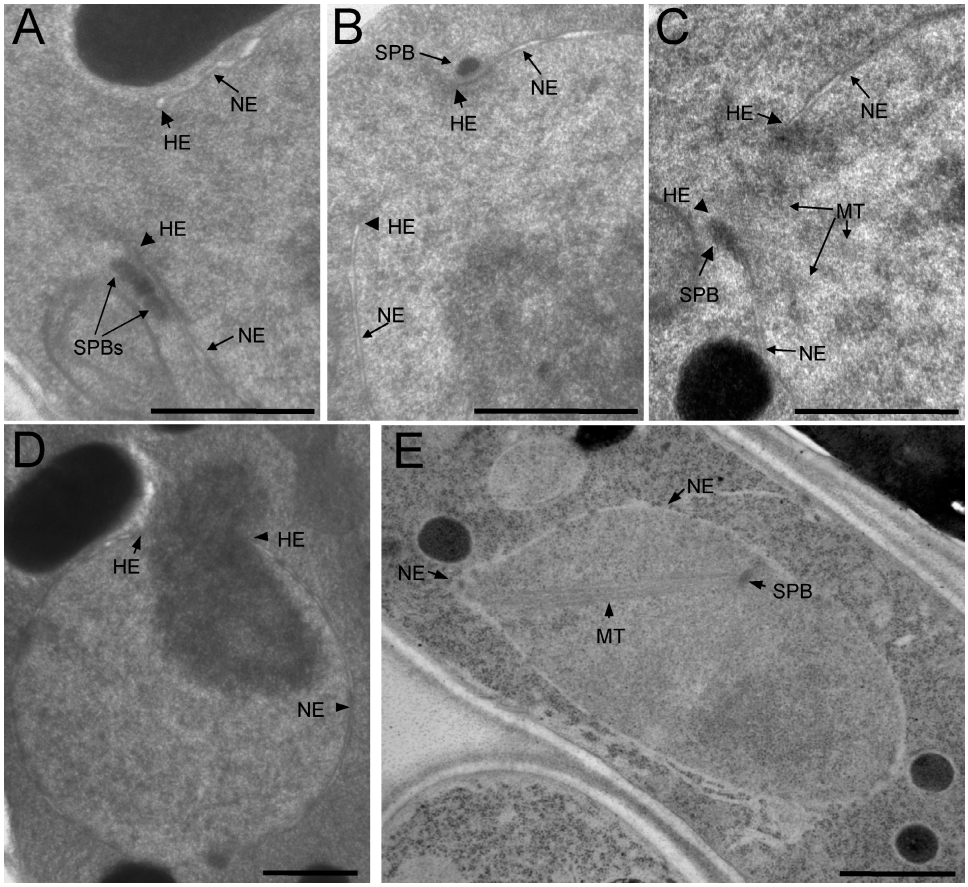

Figure 3. **Activation of the old SPB is accompanied by compromised nuclear integrity and defective SPB insertion in *cut12.1* cells at 36°C.** (A–C) Transmission electron micrographs of different nuclei where a disruption of the nuclear envelope (NE) is found next to the SPBs. (A) Two SPBs linked by the bridge structure. (B) A single noninserted SPB adjacent to a large hole in the envelope. (C) The cell is clearly in mitosis, as microtubules (MT) emerge from the SPB adjacent to the hole in a characteristic V-shape monopolar fashion. (D) Nucleoplasm leaking into the cytoplasm. (E) An example of an active SPB that has fallen into the nucleus. Note the herniation of the membrane arising from the polymerization of microtubules from this SPB to a point on the membrane that is devoid of an SPB. Similar images arise in *cut11* mutant mitoses (West et al., 1998). HE, hole edge. Bars, 500 nm.

before fixation but that membrane disruption was induced during processing. Therefore, we decided to study the integrity of the nuclear envelope. We used a well-characterized nuclear marker, the NLS-GFP–β-galactosidase (β-Gal) fusion protein (Yoshida and Sazer, 2004). Live cell imaging of wild-type cells that expressed a red fluorescent tubulin fusion protein (pRep81Cherry-tubulin) confirmed that the fluorescent signal of this NLS-GFP–β-Gal remained constrained within the nuclear envelope throughout the cell cycle of wild-type cells (Fig. 4 A and Video 1; Yoshida and Sazer, 2004).

Nuclear integrity is maintained when a failure to interdigitate the two half spindles arrests mitotic progression

To determine whether NLS-GFP–β-Gal was retained within the nucleus during a prolonged mitotic arrest, we blocked mitotic progression by introduction of the *cut7.24* mutation into the NLS-GFP–β-Gal pRep81Cherry-tubulin background. As *cut7*$^+$ encodes *S. pombe* kinesin 5, it is required for the interdigitation of the two half spindles (Hagan and Yanagida, 1990). Loss of Cut7 function activates the spindle assembly checkpoint to block mitotic progression (Kim et al., 1998). To confirm that the integrity of the nuclear envelope was not compromised by *cut7.24* mutation, we processed cells that had been arrested at the restrictive temperature for 3 h for EM. Serial sections through the nuclei of 10 cells revealed that both SPBs had integrated into the nuclear envelope and that the two half spindles had indeed failed to interdigitate in every case (Fig. 5 and Fig. S3). Consistently, the NLS-GFP–β-Gal fusion protein was retained within the nucleus throughout the mitotic arrest until the cells leaked through the cell cycle arrest and the cytokinetic ring randomly cleaved the nucleus in two in a cut phenotype (Fig. 4 B and Video 2).

Nuclear integrity is compromised in *cut12.1* and *cut11.1* arrests

As the trans-membrane motif bearing protein Cut11 is required for the integration of the SPB into the nuclear envelope (West et al., 1998), we anticipated that the *cut11.1* mutation would affect the integrity of the nuclear envelope and so would permit efflux of the NLS-GFP–β-Gal from the nucleus as they unsuccessfully attempted to integrate the SPB into their nuclear envelope. In line with this prediction, a burst of GFP fluorescence appeared throughout the cytoplasm when the red fluorescent interphase microtubules depolymerized to mark commitment to mitosis (Fig. 4 C and Video 3). The reaccumulation of this marker within the nuclei after leakage is likely caused by the presence of

Published June 1, 2009

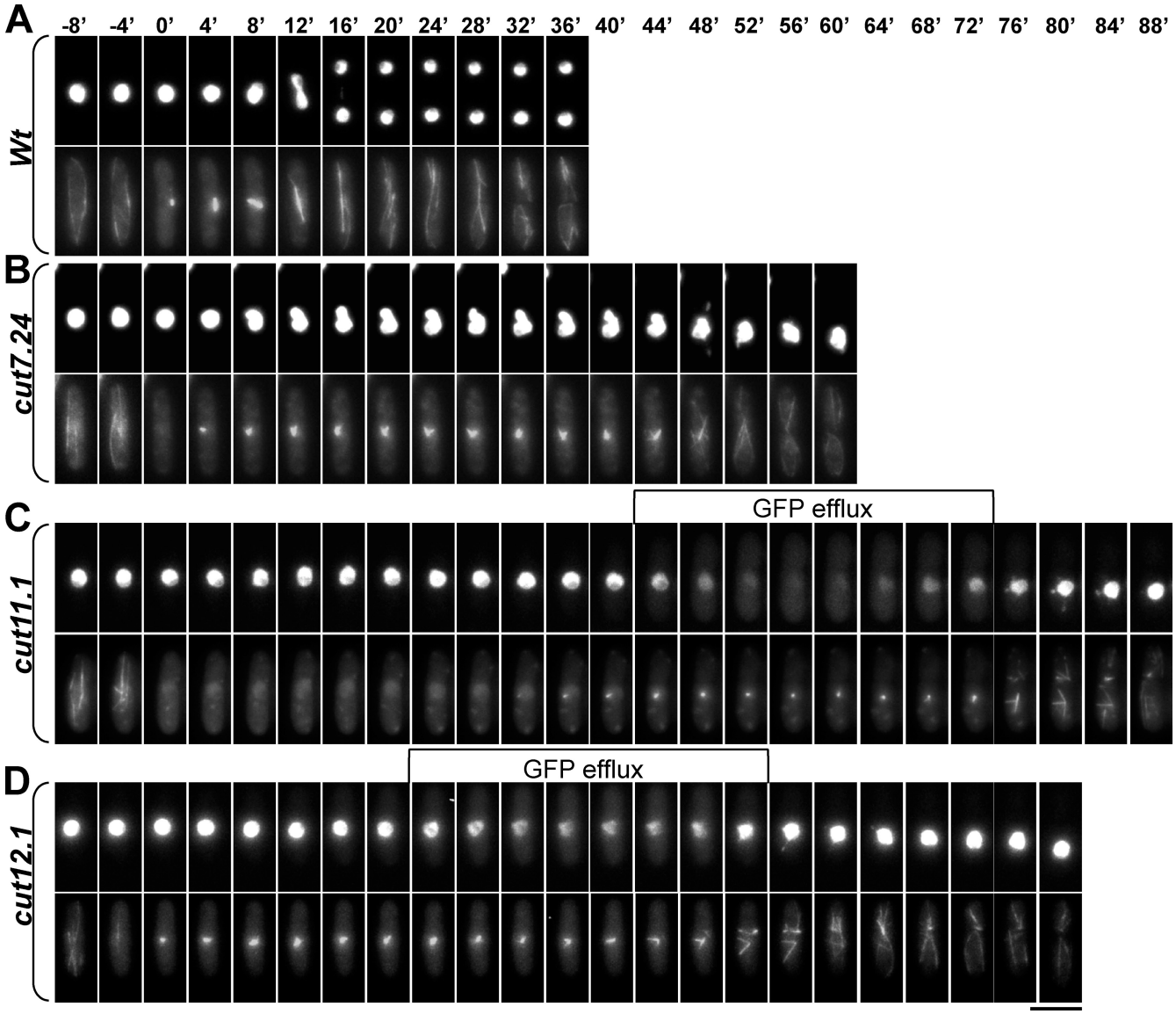

Figure 4. **Efflux of a nuclear GFP marker accompanies the defective mitosis of *cut11.1* and *cut12.1* cells at 36°C.** (A–D) Wild-type (Wt; A; Video 1), *cut7.24* (B; Video 2), *cut11.1* (C; Video 3), or *cut12.1* (D; Video 4) strains incorporating both integrated NLS-GFP–β-Gal and pRep81Cherry-tubulin plasmid were grown at 25°C and mounted for live imaging at 36°C. Time-lapse images were captured in both green (top image at each time point marker; *NLS-GFP–β-Gal* nuclear integrity marker) and red (bottom image; tubulin to image microtubules) channels every 4 min. Time 0 indicates the first time lapse in which interphase microtubules are no longer found. GFP signal leaks into the cytoplasm of mitotic (as indicated by the tubulin in the bottom panels) *cut12.1* and *cut11.1* cells (frames labeled as GFP efflux). No efflux is observed in the wild-type or *cut7.24* controls. Bar, 10 μm.

the nuclear localization signal that will drive its reimport into nuclei once the nuclear envelope is resealed and a RAN (ras-related nuclear protein) GTP gradient is reestablished.

Having established that the NLS-GFP–β-Gal marker is retained within the nuclei of cells that maintain the integrity of the nuclear envelope during mitosis but not in those in which integrity is compromised, we monitored NLS-GFP–β-Gal fluorescence in *cut12.1* cells at 36°C. 52 of the 54 cells observed formed a monopolar spindle with microtubules emanating from a single point within the cell. The formation of each of these monopolar spindles was accompanied by a brief efflux of GFP signal from the nuclei (Fig. 4 D and Video 4). Thus, the compromised Cut12 function of the *cut12.1* allele disrupted the integrity of the nuclear envelope as cells attempted to form a spindle. This would explain our ability to identify cells in which an active SPB had apparently lost its association with the membrane completely and fallen into the middle of the nucleus (Fig. 3 E) and the proximity of the SPB to these gaps in the membrane (Fig. 3, A–C).

cut12.1 and *cut11.1* mutations delay SPB activation during commitment to mitosis

The visualization of microtubules in the *cut12.1*, *cut11.1*, and *cut7.24* backgrounds to monitor the timing of commitment to mitosis revealed an additional defect in SPB activation during mitotic commitment in *cut11.1* and *cut12.1* cells. The dissolution of cytoplasmic interphase microtubules is either coincident with or rapidly followed by (within 4 min) the nucleation of spindle microtubules from the mitotic SPBs when wild-type or

Published June 1, 2009

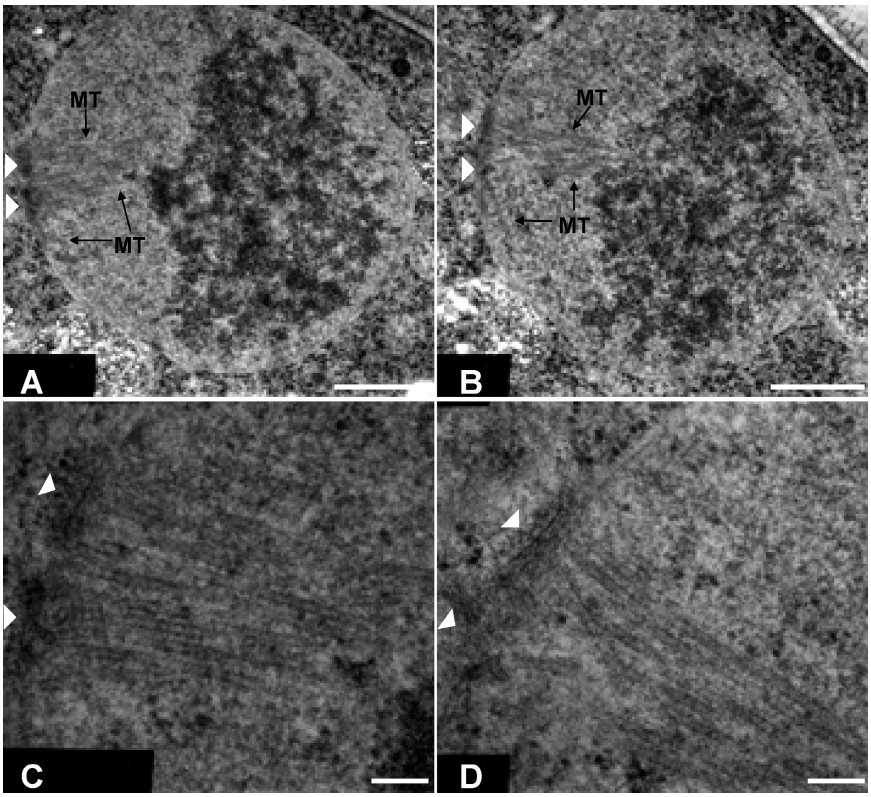

Figure 5. **SPB insertion in *cut7.24* mutant cells at 36°C.** *cut7.24* cells were grown at the permissive temperature until early-log phase when they were shifted to the restrictive temperature. 3 h later, samples were taken for transmission EM processing. (A–D) Micrographs of two consecutive sections of a mitotic nucleus are shown (A and B) alongside enlargements of relevant areas of both (C and D). In contrast to *cut12.1* cells, both SPBs insert into the nuclear envelope. Microtubules (MT) from both SPBs run parallel and fail to interdigitate. White arrowheads indicate the SPBs. Bars: (A and B) 500 nm; (C and D) 100 nm.

cut7.24 cells commit to mitosis (Fig. 6, A, B, and E). In contrast, the timing of spindle appearance in *cut12.1* and *cut11.1* mutants was highly variable. In just 2 out of the 15 cells examined, the spindle formed immediately upon the dissolution of interphase microtubules, whereas in the remainder, spindle microtubules failed to appear for up to 2 h after the interphase microtubules had depolymerized (Fig. 6, C–E). We conclude that the failure of the new SPB to activate in *cut12.1* is accompanied by an inability of the old SPB to integrate appropriately into the nuclear envelope and significant delays in the activation of this old SPB.

Elevation of Cdc25 levels is unable to suppress the lethality or spindle formation defects of *cut11.1*

Given the striking similarities between the *cut12.1* and *cut11* mutant phenotypes and the synthetic lethality arising from combining both mutations in one cell (West et al., 1998), we assessed how far this similarity extended. Specifically, we asked whether the elevation of Cdc25 levels that can suppress *cut12.1* mutation (Tallada et al., 2007) could also suppress any of the *cut11.1* temperature-sensitive phenotypes. In striking contrast to the rescue of the *cut12.1* defect, elevation of Cdc25 arising from integration of the *cdc25.d1* allele at the *leu1* locus (Daga and Jimenez, 1999; Tallada et al., 2007) did not enable *cut11.1* cells to overcome their spindle formation defect and grow at 36°C (Fig. 7 A). Likewise, although increasing Cdc25 levels led to a greater than fourfold reduction in the cut phenotype that accompanies defective mitosis in *cut12.1*, no significant reduction of this defect was observed in *cut11.1* (Fig. 7 B).

Levels of Cdc25 that suppress the spindle formation defect of *cut12.1* do not suppress the nuclear integrity defect

Because the efflux of the NLS-GFP–β-Gal marker that accompanies the defective mitosis in *cut12.1* and *cut11.1* is an uncharacterized phenotype for these mutations, we asked whether the elevation of *cdc25* levels suppressed the NLS-GFP–β-Gal efflux. To this end, we monitored wild-type, *cut12.1*, and *cut11.1* cells harboring the *cdc25.d1 NLS-GFP–β-Gal* transgenes by live cell imaging at the restrictive temperature of 36°C (Fig. 7 C). There was no significant reduction in the frequency or duration of leakage of nucleoplasm from the nuclei of *cut11.1* cells (Fig. 7, C–E). Surprisingly, in 50% (n = 79) of the *cut12.1* cells that successfully completed mitosis, an efflux of the NLS-GFP–β-Gal marker accompanied mitotic commitment (Fig. 7, C and D). However, notably, this leakage was significantly briefer than in *cut12.1* single mutant (Fig. 7 E). These data indicate that the level of Cdc25 activity required to suppress the SPB activation and insertion defect of the new SPB is below the threshold required to ensure a high fidelity of integration into the nuclear envelope. Thus, two distinct stages of nuclear remodeling can be differentiated by the *cut12.1* mutation: SPB activation and correct integration of the activated SPBs within the nuclear envelope.

Discussion

We show that incubation of cells bearing the temperature-sensitive *cut12.1* mutation at 36°C blocked both the activation and insertion of the new SPB into the nuclear envelope and compromised the fidelity with which the active old SPB inserted (Fig. 8).

Published June 1, 2009

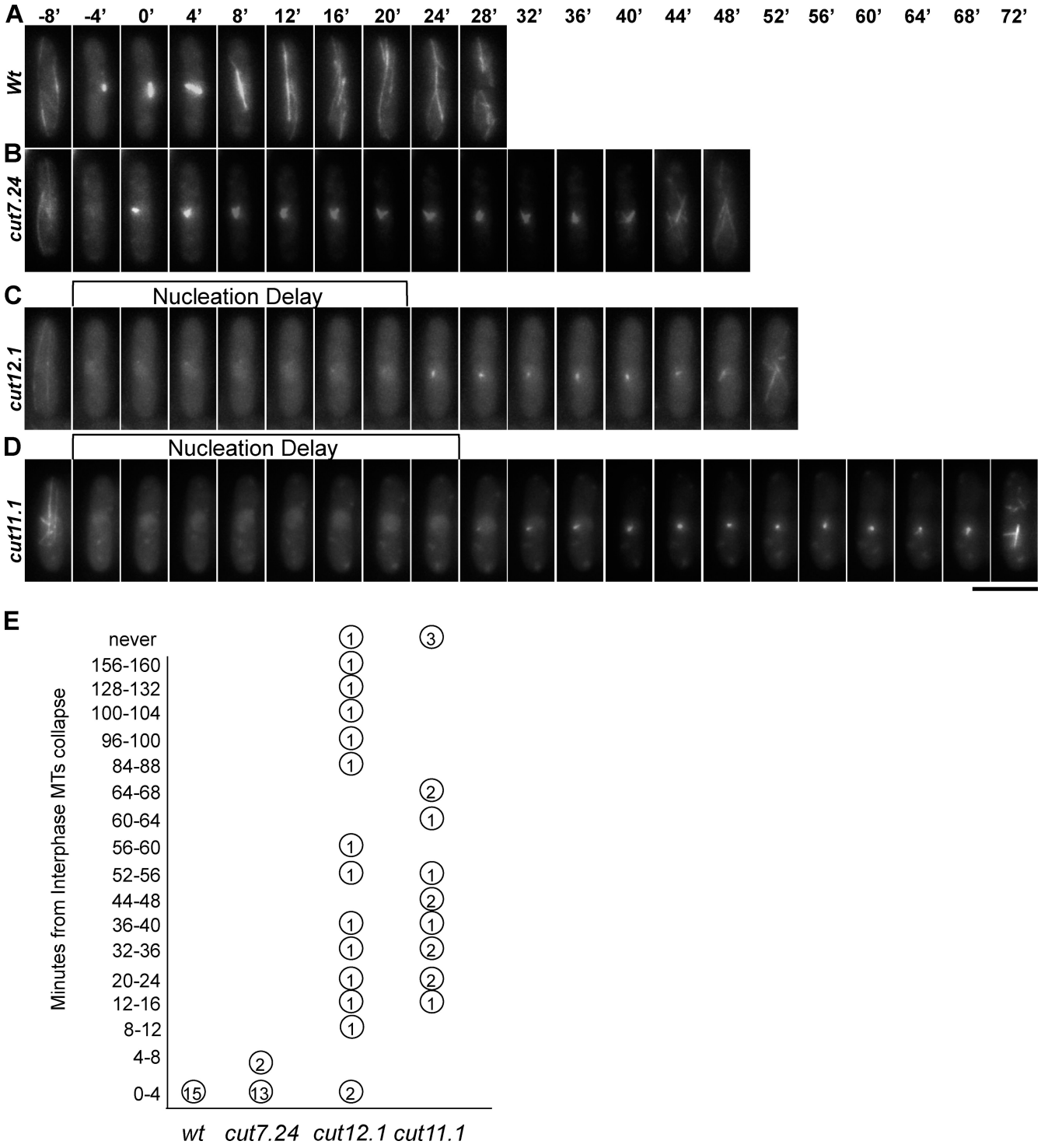

Figure 6. **Activation of the old SPB is delayed in *cut12.1* and *cut11.1* mutants.** (A–D) Wild-type (Wt) *nmt81.atb2GFP* (A; Video 1), *cut7.24 nmt81.atb2GFP* (B; Video 2), *cut12.1 nmt81.atb2GFP* (C; Video 3), or *cut11.1 nmt81.atb2GFP* (D; Video 4) cells were grown at 25°C and mounted for live imaging at 36°C. Images were captured every 4 min, and the time between the dissolution of the interphase microtubules and nucleation of mitotic microtubules was scored and plotted in E. (E) Numbers inside the circles correspond to the number of individual cells that spent this specific time interval (y axis) without microtubules (MT). For each strain, $n = 15$. Bar, 10 µm.

The defective insertion of the old SPB was associated with leakage of nucleoplasm into the cytoplasm through gapped membrane distortions in the nuclear envelope. When an SPB was seen in the same electron microscopic section as a gap in the nuclear envelope, it was adjacent to this hole, suggesting that it was the defective attempt at SPB insertion that generated the breach in integrity. Consistently, we observed instances in which the active old SPB resided within the nucleoplasm, suggesting that it had fallen through a hole generated during the abortive attempt at spindle formation. The gap in the membrane seen in *cut12.1*

Published June 1, 2009

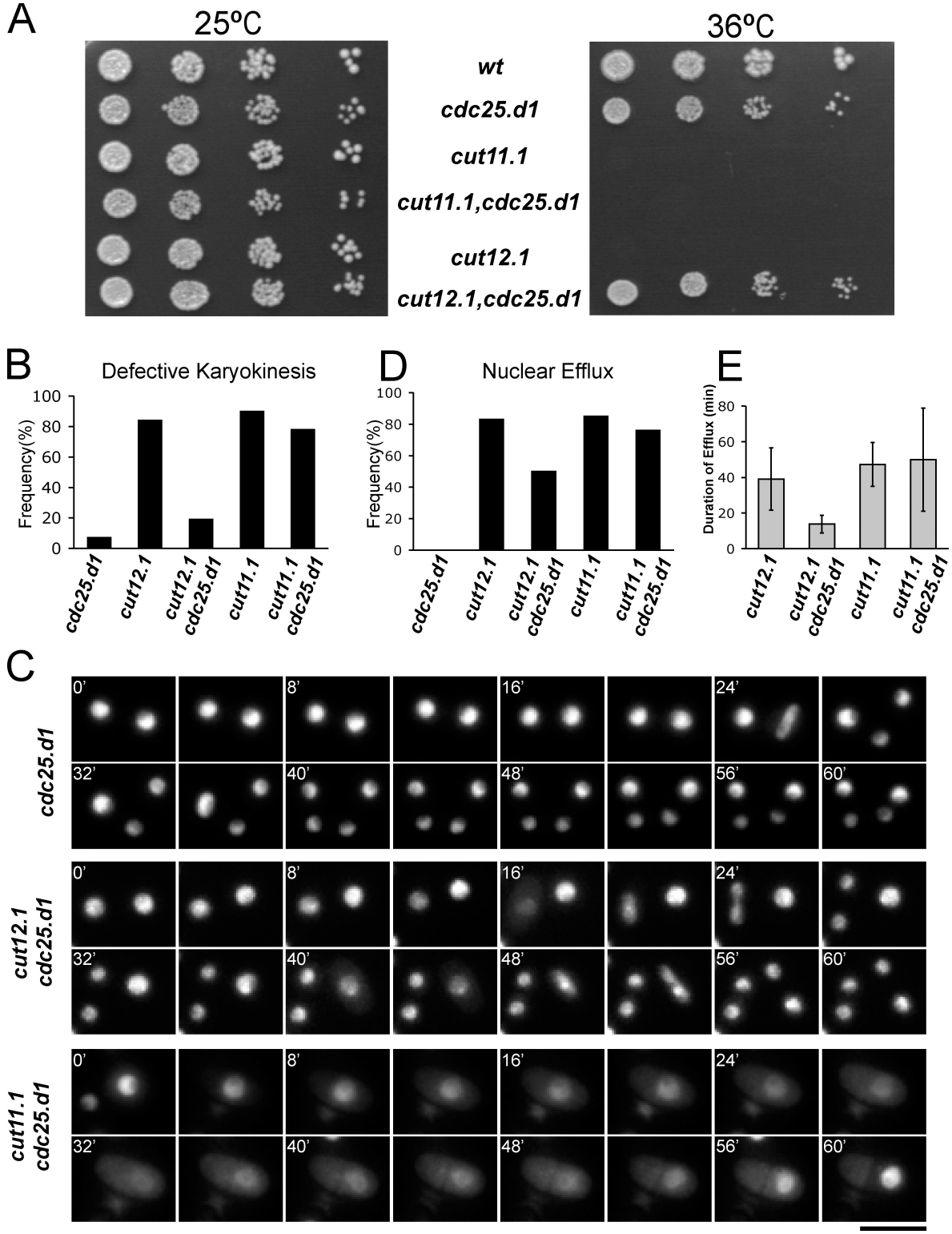

Figure 7. ***cut11.1* lethality is not rescued by boosting Cdc25.** (A) Serial dilutions (1 in 5) of the strains indicated were plated at the permissive (left) and restrictive temperature (right). In contrast to the rescue of *cut12.1* by stabilizing cdc25 mRNA (*cut12.1 cdc25.d1*), *cut11.1* lethality at 36°C is not suppressed in the same conditions (*cut11.1 cdc25.d1*). (B) Frequency of cells that display a defective karyokinesis, including the cut phenotype and asymmetric or no segregation of the nucleus ($n = 50$). (C) Indicated strains bearing NLS-GFP–β-Gal marker were grown at 25°C and mounted at 36°C for live cell imaging. Stacks of images were taken every 4 min to monitor karyokinesis. Both *cdc25.d1* control and *cdc25.d1 cut12.1* double mutant are able to divide the nucleus successfully, whereas in the majority of *cdc25.d1 cut11.1* cells, GFP signal leaks into the cytoplasm in mitosis. Note that the cells are very small because of the elevated levels of Cdc25. (D) Frequency of cells that show leakage at any point in the process of nuclear division ($n = 50$). (E) Mean duration of the nucleoplasm efflux in cells that were assessed in D ($n = 40$). Error bars show standard deviation. wt, wild type. Bar, 2 μm.

Published June 1, 2009

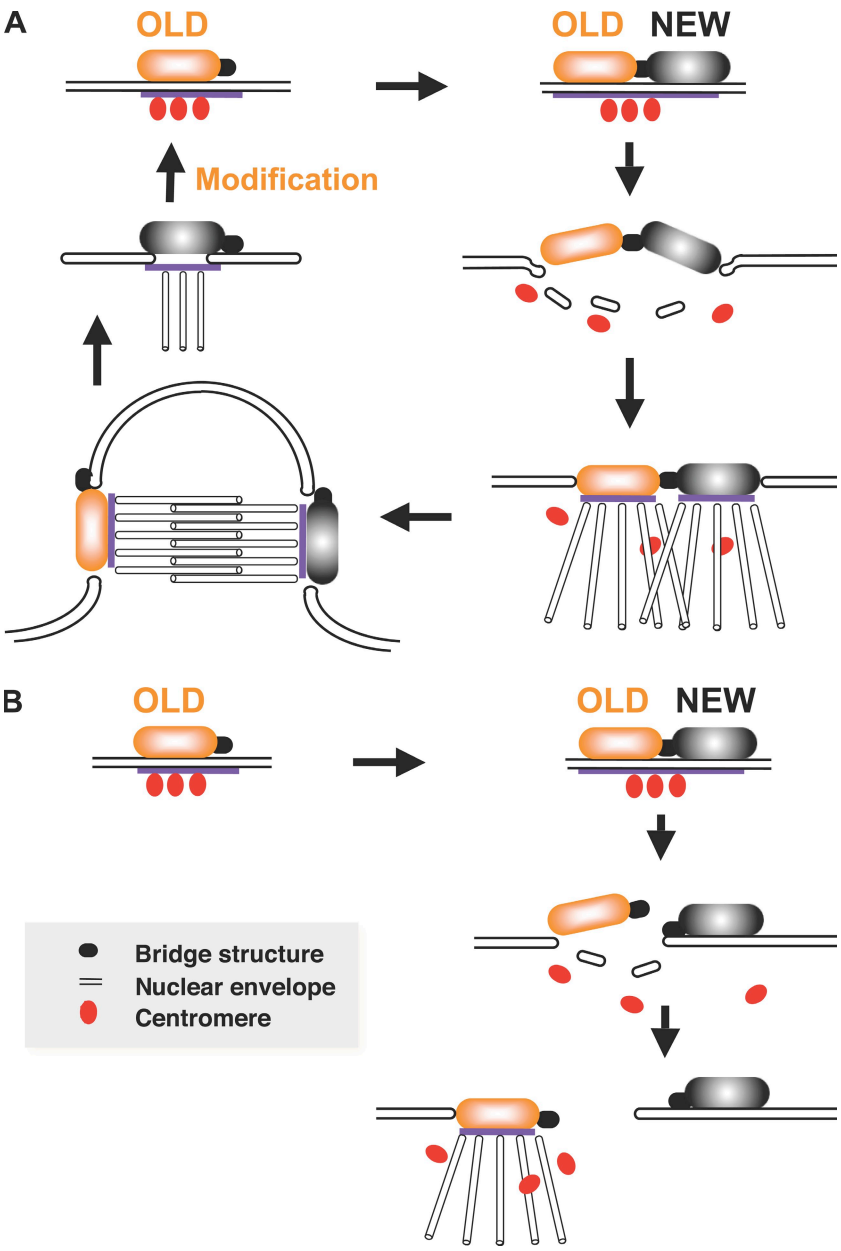

Figure 8. **A model of SPB insertion in wild-type, *cut12.1*, and *cut11.1* cells.** (A) A cartoon representing SPB integration into the nuclear envelope of wild-type cells. Note the modification that occurs during the maturation of the new SPB into an old SPB that accompanies transit through mitosis or from one cell cycle to the next (Grallert et al., 2004). (B) A cartoon representing the defective SPB integration of *cut12.1* cells.

cells greatly exceeded that of the fenestra that normally forms in the nuclear envelope for SPB insertion, suggesting that the attempt to integrate is followed by a progressive disruption of membrane integrity.

These phenotypes are highly reminiscent of those arising from mutation of the *cut11* gene. *cut11*$^{+}$ encodes a protein with six or seven predicted trans-membrane domains that associate with the nuclear pores in interphase and both the nuclear pores and SPBs of mitotic cells (West et al., 1998; Stavru et al., 2006). It is the functional homologue of the budding yeast Ndc1p protein (Winey et al., 1993; West et al., 1998). In *cut11.1* mutant cells, the old SPB nucleates microtubules, whereas the new SPB remains inactive. This old SPB can fail to associate with the nuclear envelope and, like the *cut12.1* mutant SPB we describe in this study, can fall into the heart of the nucleoplasm (West et al., 1998). Sad1 often preferentially associated with the inactive SPB in both *cut11* and *cut12* mutants.

Despite these striking similarities between the *cut11* and *cut12* mutant phenotypes, the genetic relationship of *cut11.1* with an integrated version of the *cdc25.d1* allele that elevates the levels of Cdc25 to promote premature mitosis (Daga and Jimenez, 1999; Tallada et al., 2007) was different. Elevation of Cdc25 levels to boost MPF activity promoted the activation of the otherwise inactive new SPB in the majority of *cut12.1* cells. In contrast, the presence of *cdc25.d1* had no impact on the spindle formation or abnormal mitotic or temperature-sensitive lethality phenotypes of the *cut11.1* mutation. Although this distinction is based on the analysis of a single allele, it would be consistent with the view that Cut11 is a physical component of the SPB that is required to generate an interface through which the proteinaceous SPB becomes an integral part of the nuclear envelope, whereas Cut12 is a regulatory protein that is required for SPB activation and the control of mitotic commitment.

Published June 1, 2009

Because MPF is recruited to the SPBs of late G2 cells (Alfa et al., 1990; Decottignies et al., 2001), we propose that the compromised Cut12 function of *cut12.1* cells reduced the activation of MPF on the new SPB below the critical threshold required for SPB integration into the membrane (Figs. 8 and 9). The elevation of global Cdc25 levels via the introduction of the *cdc25.d1* allele then raised global MPF activity to drive the local level at the SPB back above the threshold for, and so restored, SPB integration. The morphology of the nuclear envelope underlying the cytoplasmic SPB component of the inactive SPB in *cut12.1* mutants supports this view of defective MPF at the new SPB, as it retains the differentiated appearance that is the hallmark of an interphase SPB (Ding et al., 1997).

The restriction of the SPB activation/integration defect to one of the two SPBs suggests that Cut12 acts in cis in a local fashion on individual SPBs to promote MPF activation at individual SPBs, which drives integration of the SPB into the membrane (Fig. 9, red arrows), whereas the ability of the dominant *cut12.s11* mutation to permit division of *cdc25.Δ* and *cdc25.22* cells in a polo-dependent fashion (Hudson et al., 1990, 1991; MacIver et al., 2003) suggests that these events on the SPB are amplified and harnessed by different pathways to influence the global control of mitotic commitment (Fig. 9, green arrows). Such global control from a defined structure echoes the mechanism by which a single unattached kinetochore arrests cell cycle progression (Musacchio and Salmon, 2007). This proposed importance of SPB-associated events in regulating mitotic commitment in fission yeast is supported by the observation that constitutively active Plo1 kinase is only able to suppress *cdc25.22* mutants when it is able to associate with the SPB (Petersen and Hagan, 2005).

Elevating Cdc25 levels suppressed the efflux of the NLS-GFP–β-Gal nuclear marker to a lesser degree than it suppressed the SPB activation and insertion defect. This suggests that SPB activation is regulated in a manner that is distinct from the controls that govern membrane insertion. A further striking feature of the efflux of the GFP marker was the speed with which the GFP nuclear marker reaccumulated in the nuclei after efflux in *cut12.1* and *cut11.1* cells. Current technologies have not allowed us to address the duration of the different phases of rupture, repair (assuming that there is repair), and reimport. It is possible that the breach of the nuclear envelope is very transient, after which it takes 40 min to reimport the entire population of NLS-GFP–β-Gal back into the nucleus, or that the rupture persists but that the RAN GTP system can establish a gradient that is sufficient to direct import even though membrane integrity is compromised at one point. Given the size of the breach to the nuclear envelope recorded in images such as that in Fig. 3 D, it is hard to imagine how the nuclear envelope could reseal. In this respect, it may be important to consider the distinctions between the point at which *cut7* and *cut12* mutant cells loose viability as they undergo a defective mitosis. The death of *cut7.446* cells coincides with the inability to form the mitotic spindle, whereas the viability of *cut12.1* cells has already fallen to 60% of its starting value by the time that the first spindle appears (Hagan and Yanagida, 1990, Bridge et al., 1998). This may indicate that although the NLS-GFP–β-Gal reaccumulates within the nuclei after efflux, there is lasting damage to nuclear integrity. This would favor the interpretation that the RAN GTP system can accommodate a moderate perturbation of nuclear cytoplasmic partitioning.

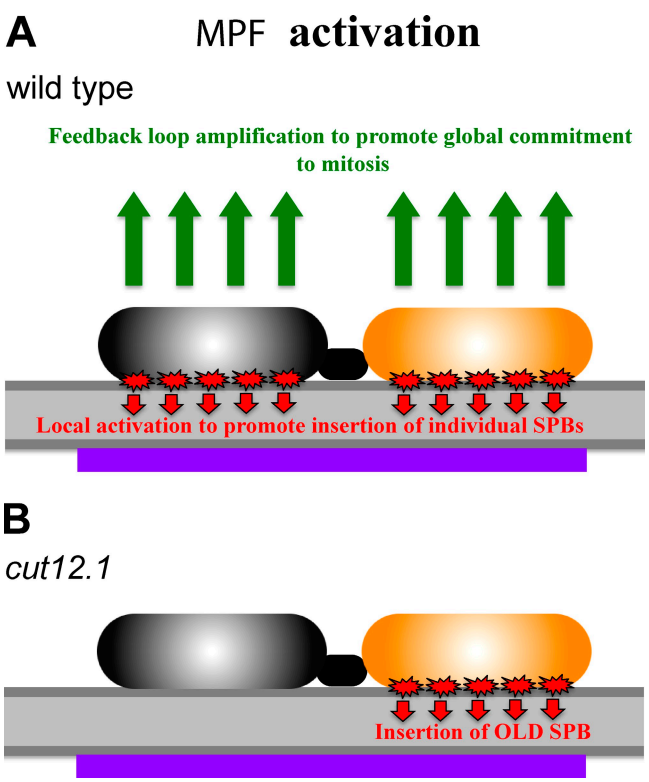

Figure 9. **A model depicting the proposed distinctions between local and global MPF activation in wild-type and *cut12.1* cells.** The cartoons show the two types of signaling event that we believe the *cut12.1* mutant phenotype and relationship between *cut12*$^+$ and *cdc25*$^+$ have revealed. (A) In addition to a global signaling event that commits the cell to mitosis (green), we propose that local activation of MPF (red) is required on individual SPBs to promote the insertion of these SPBs into the nuclear envelope (gray lines). (B) In *cut12.1* mutants, the old (orange) but not the new SPB (gray) is competent to promote local activation. It is unclear at present whether the signal for global commitment in *cut12.1* mutant cells comes from the old or new SPB, so this signal is omitted from this panel.

Sad1 often preferentially associates with the inactive new SPB in both *cut11.1* and *cut12.1* mutant cells (Fig. 2 B; Bridge et al., 1998). This asymmetry reflects the membrane association of the two SPBs. Like all SUN domain proteins that anchor MTOCs to the nuclear envelope (Tzur et al., 2006; Wilhelmsen et al., 2006), the trans-membrane domain of Sad1 gives it an intrinsic affinity for the nuclear envelope (Hagan and Yanagida, 1995). If this affinity were to be greater than its affinity for the SPB, Sad1 would preferentially partition with the inactive, membrane-associated rather than the active, membrane-free SPB. In contrast to *cut12.1,* a complete loss of Cut12 function arising from deletion of the *cut12*$^+$ gene results in two equally staining Sad1 foci with microtubules emanating from another site within the heart of the nucleoplasm (Bridge et al., 1998). It is tempting to speculate that the complete absence of Cut12 protein from these germinating spores blocks the dissolution of the nuclear envelope within both SPBs, leaving the nuclear component to become active, nucleate microtubules, and drift away from the sites at which the cytoplasmic domains remain associated with the nuclear envelope. The asynchrony of germination of spores makes it impractical to address this phenotype by

Published June 1, 2009

EM of germinating *cut12.d1* spores; however, it maybe possible to address this in the future, should conditional mutants that mimic this phenotype arise in future analyses of Cut12 function.

Interpreting the significance of the appearance of monopolar spindles in the first cell division after G2 cells are shifted to the restrictive temperature relies on a concrete understanding of when SPB duplication occurs. If SPB duplication occurs in G1 phase, the data suggest that there is an intrinsic difference in the response of the two SPBs to the compromised Cut12 activity. However, if the SPB duplicates in G2 phase, it may simply be that the SPB that forms after the shift to the restrictive temperature failed to incorporate sufficient functional Cut12 and so was unable to function, whereas the molecular interactions within the older SPB enabled it to retain function. The fact that Cut11 only associates with the SPB upon mitotic commitment and yet *cut11* mutants have a monopolar phenotype (West et al., 1998) argues that it arises from an intrinsic difference in the potential of the SPBs to cope with alterations in SPB function. This view is supported by our demonstration of an inherent functional distinction between the two anaphase B SPBs, as the septum initiation network promotes septation from the new, not the old, SPB (Sohrmann et al., 1998; Grallert et al., 2004). A recent study suggests that these distinctions are established by G2 phase, as the KASH (Klarsicht/ANC-1/Syne-1 homology) domain protein Kms2 associated with only one of the two Sad1-staining SPBs in *ima1.Δ* mutants (King et al., 2008). Furthermore, Fin1 association with SPBs shows that, just like metazoan centrioles (Vorobjev and Chentsov, 1982), a novice *S. pombe* SPB actually takes more than one cell cycle to fully mature (Grallert et al., 2004). In the model, to account for this SPB maturation, we proposed that passage through mitosis or G1 modifies one of the two SPBs such that its behavior in the next cell cycle is altered (Grallert et al., 2004). In other words, exposure to a mitotic environment or transit through START could modify the SPB such that its threshold requirement for Cut12 function is lower than that of the neighboring new SPB that is yet to experience these modifications (Fig. 8 A). Whatever the explanation, it is clear that there are inherent differences between the two SPBs in each cell, and it appears that Cut12 function is sensitive to these distinctions.

Live cell imaging also revealed a variable delay between the dissolution of interphase microtubules and the formation of the mitotic spindle when the integrity of the nuclear envelope was compromised by either the *cut11* or *cut12* mutations. This delay may arise from altered partitioning of key cell cycle regulators between the cytoplasm and nucleoplasm or the leakage of critical spindle components, such as tubulin from the mitotic nuclei through the gapped membrane distortions that accompany the defective mitoses in these mutants. In conclusion, we propose that Cut12 acts in cis to promote the changes that drive the integration and activation of SPBs into the nuclear envelope at the start of mitosis and globally to control the rate at which cells execute the global decision to commit to mitosis.

Materials and methods

Cell growth

Growth and maintenance of strains were performed according to Moreno et al. (1991). The strains used in this study are listed in Table S1. Strains IH1741 and IH5253 were gifts from T. Toda (Cancer Research UK London Research Institute, London, England, UK) and S. Sazer (Baylor College of Medicine, Houston, TX), respectively.

EM

Plunge freeze substitution fixation and subsequent preparation of *cut7.24* cells for EM were performed according to Kanbe et al. (1989). 3 h after shift of an early-log phase culture from 25°C to 36°C, cell suspensions were dotted onto filter paper and then sandwiched between two copper grids. Fixation was achieved by plunging into liquid propane. Subsequent substitution with anhydrous acetone containing 2% OsO_4 and 0.05% uranyl acetate took 48 h at −79°C. The temperature was then increased to −20°C for 2 h followed by 1.5 h at 4°C before incubation at room temperature for 30 min. After four washes in anhydrous acetone, step-wise infiltration with Epon-Araldite led to a final infiltration of 100%. Samples were sandwiched between Teflon-coated glass and polymerized at 70°C for 48 h. Blocks were trimmed, and serial sections were prepared with a diamond knife and mounted on Formvar-coated single-slot grids for staining with uranyl acetate and lead citrate. Images were taken with an electron microscope (100 CX; JEOL) operated at 100 kV.

High pressure freeze substitution of *cut12.1* cells was performed as described previously (Murray, 2008). *cut12.1* cells were synchronized with respect to cell cycle progression by centrifugal elutriation according to Creanor and Mitchison (1979) using an elutriator rotor (JE-5.0; Beckman Coulter). After filtration onto 0.45-µm membrane filters (Millipore), cells were loaded into interlocking brass hats (Swiss Precision) and fixed by high pressure freezing with a high pressure freezer (HPM010; Bal-Tec). Freeze substitution into 2% OsO_4 + 0.1% uranyl acetate in anhydrous acetone was conducted using an automatic freeze substitution chamber unit (AFS; Leica) at 90°C for 72 h with a 5°C h^{-1} slope to raise the temperature to −20°C, at which point cells were held for 2 h before a final increase to 4°C for 4 h at a rate of 5°C h^{-1}. After infiltration with Spurr's resin, blocks were trimmed, and serial sections were prepared with a diamond knife, mounted on Formvar/carbon-coated single-slot grids, stained with Reynolds's solution for 5 min, and imaged on a transmission electron microscope (model 1220; JEOL) at 80 kV.

Live cell microscopy

Live cell image capture and analysis were performed according to Grallert et al. (2006). Cells were grown in supplemented, filter-sterilized EMM2 at 25°C before being mounted on an FCS2 chamber (Bioptechs) coated with soybean lectin (Sigma-Aldrich). The chamber was mounted onto a Deltavision Spectris system (Applied Precision, LLC) that uses a microscope (IX71; Olympus). The Precision Control Weather Station heating chamber (Applied Precision, LLC) surrounding the stage and the FCS2 chamber were set at 36°C as was the objective heating collar (Bioptechs) on the 100× NA 1.45 objective (Carl Zeiss, Inc.) that was used to capture images. This led to a temperature shift of the cells from 25 to 36°C in 2 min after mounting on the microscope. Image capture started once the focus had stabilized (45 min). 20 0.3-µm consecutive slices were captured every 4 min with a camera (Cascade II 512b; Photometrics) using the SoftWoRx (Applied Precision, LLC) image capture program. The Z series was then compressed to a maximal projection in Imaris software (Bitplane). Individual panels were extracted into Photoshop (Adobe) to generate the panels for the figures.

Immunofluorescence microscopy

Immunofluorescence microscopy was performed according to Hagan and Yanagida (1995), in which the TAT1 anti–α-tubulin monoclonal antibody (Woods et al., 1989) that was used at a dilution of 1 in 80 was detected with FITC-conjugated goat anti–mouse IgG (Sigma-Aldrich) and the cAP9.5 anti-Sad1 antibody that was used at a dilution of 1 in 25 was detected with CY3-conjugated goat anti–rabbit IgG antibody (Sigma-Aldrich). Samples were imaged and processed as for live imaging with the exception that cells were mounted on soybean lectin–coated, standard 18 × 18–mm 1.5 coverslips and no heating of the sample was used. pRep81Cherry-tubulin was a gift from K. Tanaka (University of Leicester, Leicester, England, UK).

Online supplemental material

Fig. S1 shows further detail of the cell shown in Fig. 1. Fig. S2 shows a second example of electron microscopic sections from a *cut12.1* cell in which one SPB is active and nucleating microtubules, whereas the structure of the second SPB is highly reminiscent of the structure of a wild-type interphase SPB in which the cytoplasmic component associates with the outside of the nuclear envelope. Fig. S3 shows a second example of EM analysis of a *cut7.24* cell to show the two active SPBs inserted into a continuous nuclear envelope. Videos 1 and 2 show the retention of the NLS-GFP–β-Gal nuclear integrity marker in wild-type and *cut7.24* mitoses, respectively.

Videos 3 and 4 show the transient efflux of this marker as *cut11.1* and *cut12.1* cells, respectively, transit mitosis. Table S1 lists the strains used in this study. Online supplemental material is available at http://www.jcb.org/cgi/content/full/jcb.200812108/DC1.

We thank Steve Bagley of the Paterson Advanced Imaging Facility and Stephen Murray of the Electron Microscopy Facility for technical support. We also thank Takashi Toda, Kayoko Tanaka, and Shelley Sazer for reagents.

This work was supported by Cancer Research UK grant C147/A6058, grants from the Human Frontier Science Program and Japan Society for the Promotion of Science, and the Spanish Government Ministerio de Ciencia e Innovación grant JC2008-00017.

Submitted: 17 December 2008
Accepted: 8 May 2009

References

Adams, I.R., and J.V. Kilmartin. 2000. Spindle pole body duplication: a model for centrosome duplication? *Trends Cell Biol.* 10:329–335.

Alfa, C.E., B. Ducommun, D. Beach, and J.S. Hyams. 1990. Distinct nuclear and spindle pole body populations of cyclin-cdc2 in fission yeast. *Nature*. 347:680–682.

Bähler, J., A.B. Steever, S. Wheatley, Y.L. Wang, J.R. Pringle, K.L. Gould, and D. McCollum. 1998. Role of polo kinase and Mid1p in determining the site of cell division in fission yeast. *J. Cell Biol.* 143:1603–1616.

Bridge, A.J., M. Morphew, R. Bartlett, and I.M. Hagan. 1998. The fission yeast SPB component Cut12 links bipolar spindle formation to mitotic control. *Genes Dev.* 12:927–942.

Chial, H.J., M.P. Rout, T.H. Giddings, and M. Winey. 1998. *Saccharomyces cerevisiae* Ndc1p is a shared component of nuclear pore complexes and spindle pole bodies. *J. Cell Biol.* 143:1789–1800.

Creanor, J., and J.M. Mitchison. 1979. Reduction of perturbations in leucine incorporation in synchronous cultures of *Schizosaccharomyces pombe* made by elutriation. *J. Gen. Microbiol.* 112:385–388.

Daga, R.R., and J. Jimenez. 1999. Translational control of the Cdc25 cell cycle phosphatase: a molecular mechanism coupling mitosis to cell growth. *J. Cell Sci.* 112:3137–3146.

Decottignies, A., P. Zarzov, and P. Nurse. 2001. In vivo localisation of fission yeast cyclin-dependent kinase cdc2p and cyclin B cdc13p during mitosis and meiosis. *J. Cell Sci.* 114:2627–2640.

Ding, R., K.L. McDonald, and J.R. McIntosh. 1993. Three-dimensional reconstruction and analysis of mitotic spindles from the yeast, *Schizosaccharomyces pombe*. *J. Cell Biol.* 120:141–151.

Ding, R., R.R. West, M. Morphew, and J.R. McIntosh. 1997. The spindle pole body of *Schizosaccharomyces pombe* enters and leaves the nuclear envelope as the cell cycle proceeds. *Mol. Biol. Cell*. 8:1461–1479.

Dutcher, S.K. 2003. Elucidation of basal body and centriole functions in *Chlamydomonas reinhardtii*. *Traffic*. 4:443–451.

Flory, M.R., M.M. Morphew, J.D. Joseph, A.R. Means, and T.R. Davis. 2002. Pcp1, an Spc110p related calmodulin target at the centrosome of the fission yeast *Schizosaccharomyces pombe*. *Cell Growth Differ.* 13:47–58.

Funabiki, H., I. Hagan, S. Uzawa, and M. Yanagida. 1993. Cell cycle–dependent specific positioning and clustering of centromeres and telomeres in fission yeast. *J. Cell Biol.* 121:961–976.

Goto, B., K. Okazaki, and O. Niwa. 2001. Cytoplasmic microtubular system implicated in de novo formation of a Rabl-like orientation of chromosomes in fission yeast. *J. Cell Sci.* 114:2427–2435.

Grallert, A., and I.M. Hagan. 2002. *Schizosaccharomyces pombe* NIMA-related kinase, Fin1, regulates spindle formation and an affinity of Polo for the SPB. *EMBO J.* 21:3096–3107.

Grallert, A., A. Krapp, S. Bagley, V. Simanis, and I.M. Hagan. 2004. Recruitment of NIMA kinase shows that maturation of the *S. pombe* spindle-pole body occurs over consecutive cell cycles and reveals a role for NIMA in modulating SIN activity. *Genes Dev.* 18:1007–1021.

Grallert, A., C. Beuter, R.A. Craven, S. Bagley, D. Wilks, U. Fleig, and I.M. Hagan. 2006. *S. pombe* CLASP needs dynein, not EB1 or CLIP170, to induce microtubule instability and slows polymerization rates at cell tips in a dynein-dependent manner. *Genes Dev.* 20:2421–2436.

Hagan, I., and M. Yanagida. 1990. Novel potential mitotic motor protein encoded by the fission yeast *cut7*$^{+}$ gene. *Nature*. 347:563–566.

Hagan, I., and M. Yanagida. 1995. The product of the spindle formation gene *sad1*$^{+}$ associates with the fission yeast spindle pole body and is essential for viability. *J. Cell Biol.* 129:1033–1047.

Hagan, I.M., and J.S. Hyams. 1988. The use of cell-division cycle mutants to investigate the control of microtubule distribution in the fission yeast *Schizosaccharomyces pombe*. *J. Cell Sci.* 89:343–357.

Hagan, I.M., and J. Petersen. 2000. The microtubule organizing centers of *Schizosaccharomyces pombe*. *Curr. Top. Dev. Biol.* 49:133–159.

Hudson, J.D., H. Feilotter, and P.G. Young. 1990. *stf1*: non wee mutations epistatic to *cdc25* in the fission yeast *Schizosaccharomyces pombe*. *Genetics*. 126:309–315.

Hudson, J.D., H. Feilotter, C. Lingner, R. Rowley, and P. Young. 1991. *stf1*: a new supressor of the mitotic control gene *cdc25* in *Schizosaccharomyces pombe*. *Cold Spring Harb. Symp. Quant. Biol.* 56:599–604.

Jaspersen, S.L., and M. Winey. 2004. The budding yeast spindle pole body: structure, duplication, and function. *Annu. Rev. Cell Dev. Biol.* 20:1–28.

Kanbe, T., I. Kobayashi, and K. Tanaka. 1989. Dynamics of cytoplasmic organelles in the cell-cycle of the fission yeast *Schizosaccharomyces pombe*: three-dimensional reconstruction from serial sections. *J. Cell Sci.* 94:647–656.

Kilburn, C.L., C.G. Pearson, E.P. Romijn, J.B. Meehl, T.H. Giddings Jr., B.P. Culver, J.R. Yates III, and M. Winey. 2007. New *Tetrahymena* basal body protein components identify basal body domain structure. *J. Cell Biol.* 178:905–912.

Kim, S.H., D.P. Lin, S. Matsumoto, A. Kitazono, and T. Matsumoto. 1998. Fission yeast Slp1: an effector of the Mad2 dependent spindle checkpoint. *Science*. 279:1045–1047.

King, M.C., T.G. Drivas, and G. Blobel. 2008. A network of nuclear envelope membrane proteins linking centromeres to microtubules. *Cell*. 134:427–438.

MacIver, F.H., K. Tanaka, A.M. Robertson, and I.M. Hagan. 2003. Physical and functional interactions between polo kinase and the spindle pole component Cut12 regulate mitotic commitment in *S. pombe*. *Genes Dev.* 17:1507–1523.

Malone, C.J., W.D. Fixsen, H.R. Horvitz, and M. Han. 1999. UNC-84 localizes to the nuclear envelope and is required for nuclear migration and anchoring during *C. elegans* development. *Development*. 126:3171–3181.

McCully, E.K., and C.F. Robinow. 1971. Mitosis in the fission yeast *Schizosaccharomyces pombe*: a comparative study with light and electron microscopy. *J. Cell Sci.* 9:475–507.

Moreno, S., A. Klar, and P. Nurse. 1991. Molecular genetic analysis of fission yeast *Schizosaccharomyces pombe*. *Methods Enzymol.* 194:795–823.

Mulvihill, D.P., J. Petersen, H. Ohkura, D.M. Glover, and I.M. Hagan. 1999. Plo1 kinase recruitment to the spindle pole body and its role in cell division in *Schizosaccharomyces pombe*. *Mol. Biol. Cell*. 10:2771–2785.

Murray, S. 2008. High pressure freezing and freeze substitution of *Schizosaccharomyces pombe* and *Saccharomyces cerevisiae* for TEM. *Methods Cell Biol.* 88:3–17.

Musacchio, A., and E.D. Salmon. 2007. The spindle-assembly checkpoint in space and time. *Nat. Rev. Mol. Cell Biol.* 8:379–393.

Oakley, C.E., and B.R. Oakley. 1989. Identification of gamma-tubulin, a new member of the tubulin superfamily encoded by *mipA* gene of *Aspergillus nidulans*. *Nature*. 338:662–664.

Pereira, G., T.U. Tanaka, K. Nasmyth, and E. Schiebel. 2001. Modes of spindle pole body inheritance and segregation of the Bfa1p-Bub2p checkpoint protein complex. *EMBO J.* 20:6359–6370.

Petersen, J., and I.M. Hagan. 2005. Polo kinase links the stress pathway to cell cycle control and tip growth in fission yeast. *Nature*. 435:507–512.

Petersen, J., and P. Nurse. 2007. TOR signalling regulates mitotic commitment through the stress MAP kinase pathway and the Polo and Cdc2 kinases. *Nat. Cell Biol.* 9:1263–1272.

Sohrmann, M., S. Schmidt, I. Hagan, and V. Simanis. 1998. Asymmetric segregation on spindle poles of the *Schizosaccharomyces pombe* septum-inducing protein kinase Cdc7p. *Genes Dev.* 12:84–94.

Stavru, F., B.B. Hulsmann, A. Spang, E. Hartmann, V.C. Cordes, and D. Gorlich. 2006. NDC1: a crucial membrane-integral nucleoporin of metazoan nuclear pore complexes. *J. Cell Biol.* 173:509–519.

Tallada, V.A., A.J. Bridge, P.E. Emery, and I.M. Hagan. 2007. Suppression of the *S. pombe cut12.1* cell cycle defect by mutations in *cdc25* and genes involved in transcriptional and translational control. *Genetics*. 176:73–83.

Tzur, Y.B., K.L. Wilson, and Y. Gruenbaum. 2006. SUN-domain proteins: 'Velcro' that links the nucleoskeleton to the cytoskeleton. *Nat. Rev. Mol. Cell Biol.* 7:782–788.

Uzawa, S., F. Li, Y. Jin, K.L. McDonald, M.B. Braunfeld, D.A. Agard, and W.Z. Cande. 2004. Spindle pole body duplication in fission yeast occurs at the G1/S boundary but maturation is blocked until exit from S by an event downstream of *cdc10*$^{+}$. *Mol. Biol. Cell*. 15:5219–5230.

Vardy, L., and T. Toda. 2000. The fission yeast gamma-tubulin complex is required in G1 phase and is a component of the spindle assembly checkpoint. *EMBO J.* 19:6098–6111.

Vorobjev, I.A., and Y.S. Chentsov. 1982. Centrioles in the cell cycle. 1. Epithelial cells. *J. Cell Biol.* 93:938–949.

Published June 1, 2009

West, R.R., E.V. Vaisberg, R. Ding, P. Nurse, and J.R. McIntosh. 1998. *cut11*$^{+}$: A gene required for cell cycle-dependent spindle pole body anchoring in the nuclear envelope and bipolar spindle formation in *Schizosaccharomyces pombe*. *Mol. Biol. Cell*. 9:2839–2855.

Wilhelmsen, K., M. Ketema, H. Truong, and A. Sonnenberg. 2006. KASH-domain proteins in nuclear migration, anchorage and other processes. *J. Cell Sci.* 119:5021–5029.

Winey, M., M.A. Hoyt, C. Chan, L. Goetsch, D. Botstein, and B. Byers. 1993. NDC1: a nuclear periphery component required for yeast spindle pole body duplication. *J. Cell Biol.* 122:743–751.

Woods, A., T. Sherwin, R. Sasse, T.H. MacRae, A.J. Baines, and K. Gull. 1989. Definition of individual components within the cytoskeleton of *Trypanosoma brucei* by a library of monoclonal antibodies. *J. Cell Sci.* 93:491–500.

Yoshida, M., and S. Sazer. 2004. Nucleocytoplasmic transport and nuclear envelope integrity in the fission yeast *Schizosaccharomyces pombe*. *Methods*. 33:226–238.

Published June 1, 2009

Supplemental Material JCB

Tallada et al., http://www.jcb.org/cgi/content/full/jcb.200812108/DC1

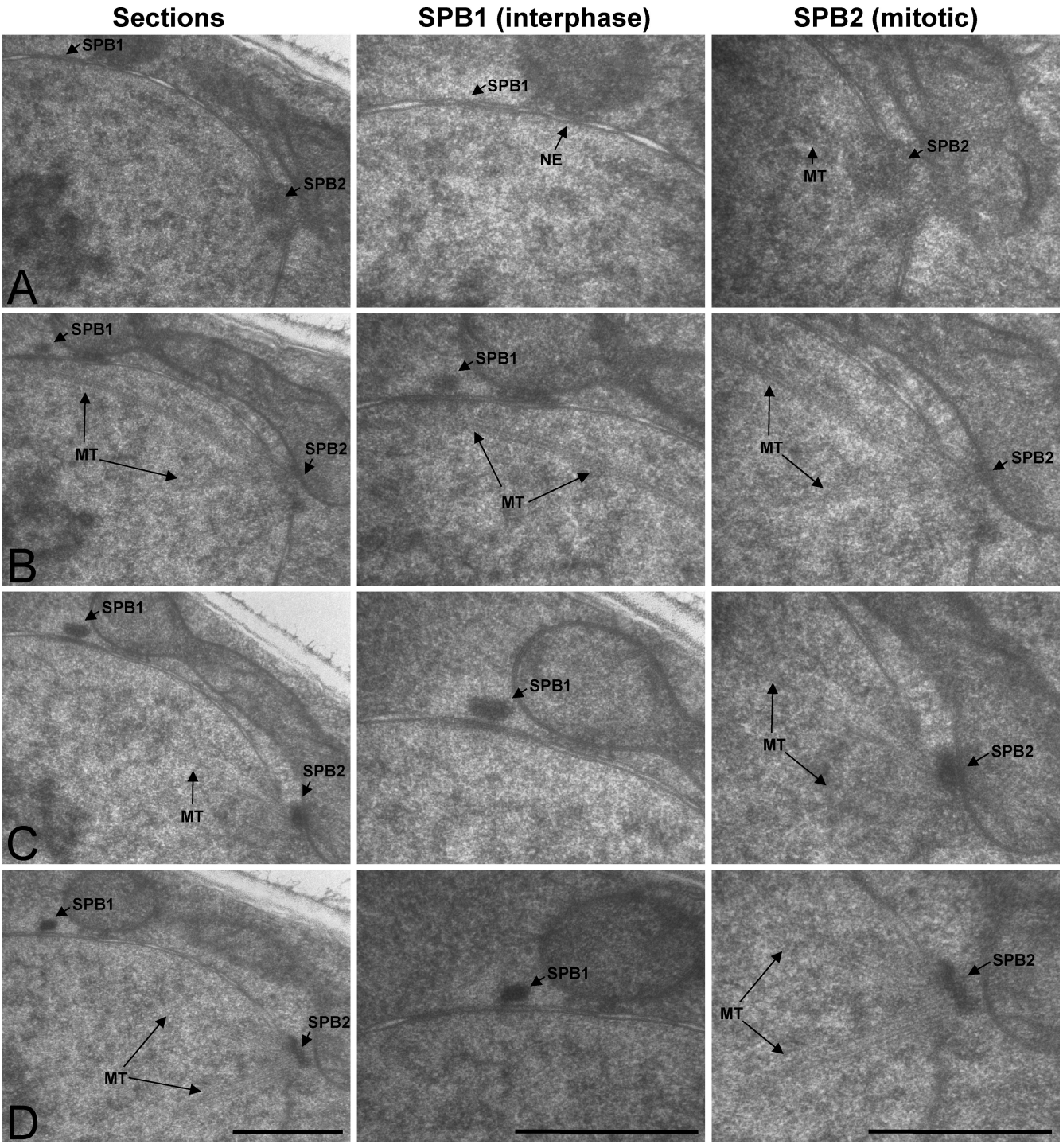

Figure S1. **Transmission electron micrographs of serial sections of *cut12.1* cells at 36°C.** (A–D) Stack of five consecutive transmission electron micrograph sections through the mitotic *cut12.1* nucleus shown in Fig. 1. The middle and right panels show enlargements of each SPB area. Note that only the correctly inserted SPB nucleates microtubules (MT). The inactive SPB retains the striations beneath the cytoplasmic structure typical of interphase SPBs. NE, nuclear envelope. Bars, 500 nm.

Published June 1, 2009

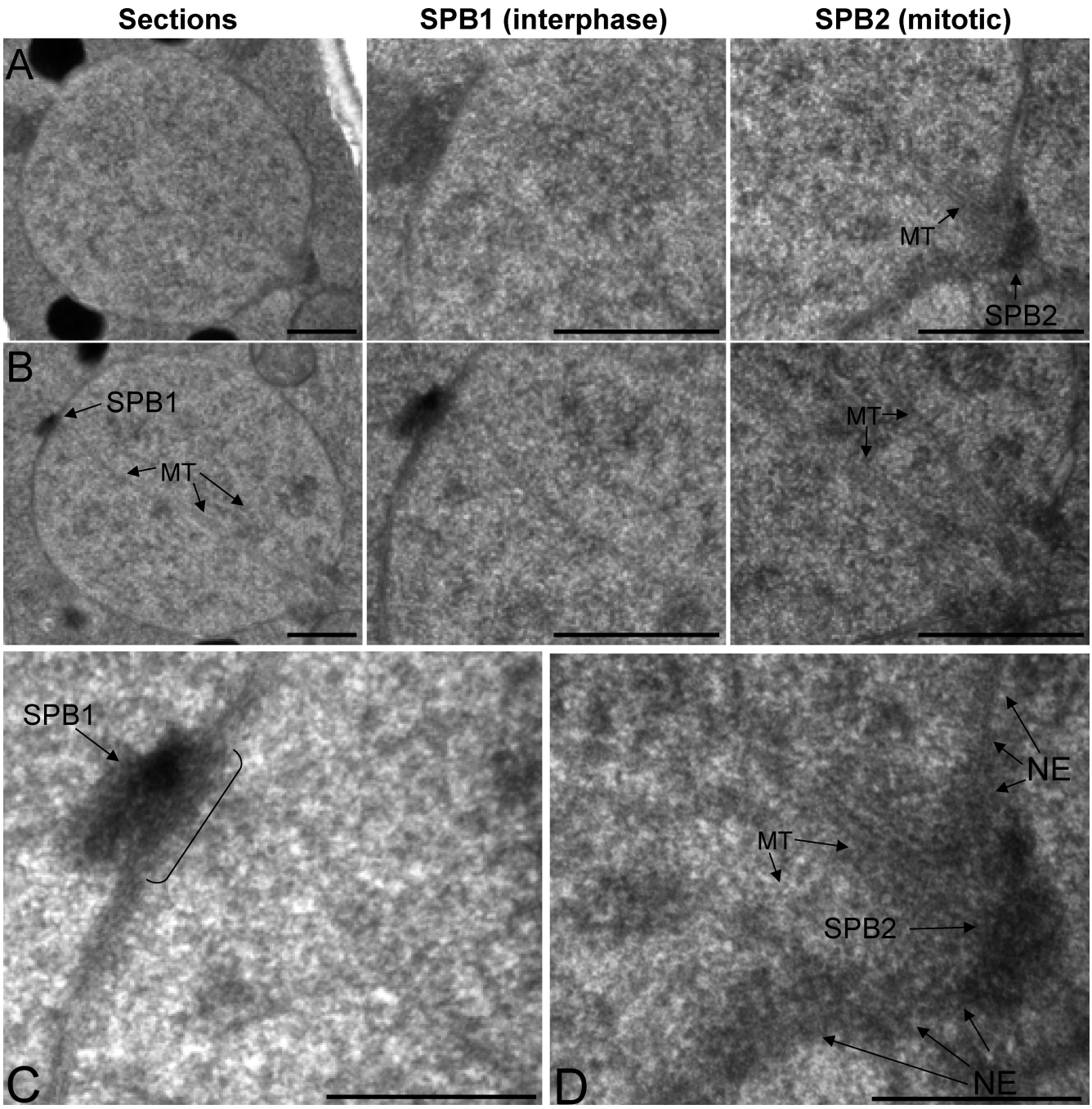

Figure S2. **Transmission electron micrographs of serial sections of *cut12.1* cells at 36°C.** (A–D) Transmission electron micrographs of two consecutive sections through a mitotic *cut12.1* nucleus. (A and B) The middle and right panels show enlargements of each SPB-containing area of the micrographs in A and B. (C and D) Further enlargement of the middle panel in B and the right panel in A, respectively. As in Fig. S1, only one SPB is integrated into the nuclear envelope (NE) to nucleate microtubules (MT; SPB2). In contrast, the nuclear envelope underneath the inactive SPB (SPB1), indicated by the bracket in C, retains the striations that are the hallmarks of an interphase SPB of wild-type cells. Bars: (A and B) 400 nm; (C and D) 100 nm.

Published June 1, 2009

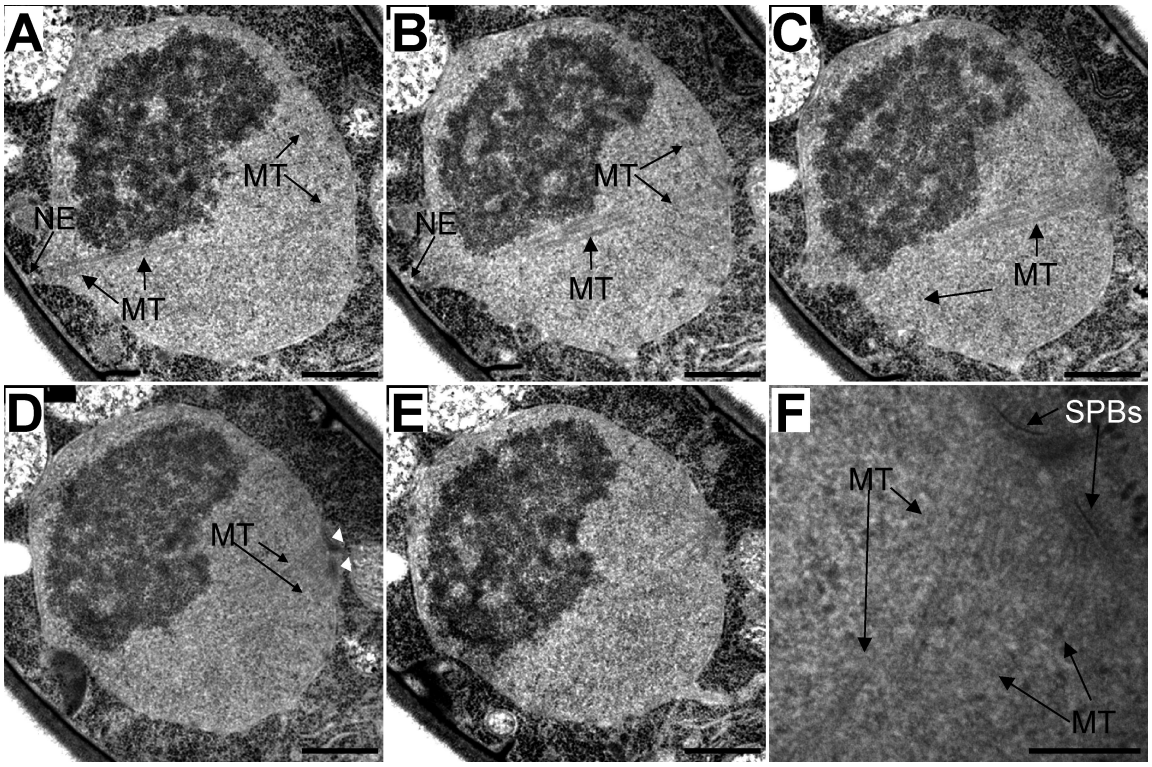

Figure S3. **Transmission electron micrographs of serial sections of *cut7.24* cells at 36°C.** (A–E) Consecutive transmission electron micrograph sections through a mitotic *cut7.24* nucleus. (F) The SPB region of section D taken at higher magnification. As in Fig. 5, both SPBs (white arrowheads in D and black arrows in F) have inserted into the nuclear envelope (NE) to nucleate microtubules (MT) that fail to interdigitate. Bars: (A–E) 500 nm; (F) 100 nm.

Published June 1, 2009

Table S1. **List of strains used in this study**

Strain	Genotype	Source
IH163	*972 h⁻*	Lab stock
IH420	*h⁺ cut12.1 leu1.32 ura4.d18 his2*	Lab stock
IH280	*h⁻ cut12.1 leu1.32*	Lab stock
IH136	*h⁻ cut7.24 leu1.32*	Lab stock
IH385	*h⁻ cut11.1 leu1.32*	West et al., 1998
IH1741	*h⁻ nmt81GFPatb2:KanMX6 leu1.32*	Garcia et al., 2001
IH7006	*h⁻ cut11.1 nmt81GFPatb2 leu1.32 ura4.d18*	This study
IH5964	*h⁻ cut7.24 nmt81GFPatb2 ura4.d18*	This study
IH5524	*h⁺ cut12.1 nmt81GFPatb2 leu1.32 ura4.d18 his2*	This study
IH2675	*h⁻ pcp1.RFP:kanR*	Lab stock
IH5012	*h⁺ cut12.1 pcp1Crfp nmt81GFPatb2:KanMX6*	This study
IH5258	*h⁻ cut12.1 int::NLS-GFP leu1.32*	This study
IH5465	*h⁺ cut12.1 nmt81GFPatb2:KanMX6 ura4.d18 his2*	This study
IH7093	*h⁻ cut11.1 pcp1Crfp nmt81GFPatb2:KanMX6*	This study
IH5253	*h⁻ SV40 NLS-GFP–β-Gal ade6.M216 leu1.32 ura4.d18*	Yoshida and Sazer, 2004
IH5429	*h⁻ SV40 NLS-GFP–β-Gal pREP81:Cherry-Tubulin leu1.32 ura4.d18*	This study
IH5430	*h⁻ cut11.1 SV40 NLS-GFP–β-Gal pREP81:Cherry-Tubulin leu1.32 ura4.d18*	This study
IH5432	*h⁻ cut12.1 SV40 NLS-GFP–β-Gal pREP81:Cherry-Tubulin leu1.32 ura4.d18*	This study
IH5433	*h⁻ cut7.24 SV40 NLS-GFP–β-Gal pREP81:Cherry-Tubulin leu1.32 ura4.d18*	This study
IH4625	*h⁻ leu1::nmt1:cdc25.d1*	Daga and Jimenez, 1999
IH4626	*h⁻ cut12.1 leu1::nmt1:cdc25.d1*	This study
IH7007	*h⁻ cut11.1 leu1::nmt1:cdc25.d1*	This study
IH7165	*h⁻ cut12.1 leu1::nmt1:cdc25.d1 SV40 NLS-GFP–β-Gal*	This study
IH7246	*h⁻ leu1::nmt1:cdc25.d1 SV40 NLS-GFP–β-Gal*	This study
IH7247	*h⁻ cut11.1 leu1::nmt1:cdc25.d1 SV40 NLS-GFP–β-Gal*	This study

References

Daga, R.R., and J. Jimenez. 1999. Translational control of the Cdc25 cell cycle phosphatase: a molecular mechanism coupling mitosis to cell growth. *J. Cell Sci.* 112:3137–3146.

Garcia, M.A., L. Vardy, N. Koonrugsa, and T. Toda. 2001. Fission yeast ch-TOG/XMAP215 homologue Alp14 connects mitotic spindles with the kinetochore and is a component of the Mad2-dependent spindle checkpoint. *EMBO J.* 20:3389–3401.

West, R.R., E.V. Vaisberg, R. Ding, P. Nurse, and J.R. McIntosh. 1998. cut11(+): a gene required for cell cycle-dependent spindle pole body anchoring in the nuclear envelope and bipolar spindle formation in *Schizosaccharomyces pombe*. *Mol. Biol. Cell.* 9:2839–2855.

Yoshida, M., and S. Sazer. 2004. Nucleocytoplasmic transport and nuclear envelope integrity in the fission yeast *Schizosaccharomyces pombe*. *Methods*. 33:226–238.

Published June 1, 2009

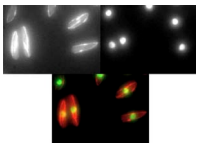

Video 1. **The NLS-GFP–β-Gal fusion protein is retained within the nucleus during mitosis of wild-type cells.** Cells incorporating both integrated NLS-GFP–β-Gal and pRep81Cherry-tubulin plasmid were grown at 25°C and mounted for live imaging at 36°C. Time-lapse images were captured in both green and red channels every 4 min. The video is shown at 3 frames/s. Panels: top left, tubulin; top right, NLS-GFP–β-Gal; bottom, merge with NLS-GFP–β-Gal in green and tubulin in red.

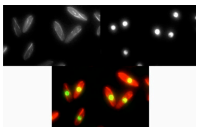

Video 2. **The NLS-GFP–β-Gal fusion protein is retained within the nucleus during mitosis of *cut7.24* cells.** *cut7.24* cells incorporating both integrated NLS-GFP–β-Gal and pRep81Cherry-tubulin plasmid were grown at 25°C and mounted for live imaging at 36°C. Time-lapse images were captured in both green and red channels every 4 min. The video is shown at 3 frames/s. Panels: top left, tubulin; top right, NLS-GFP–β-Gal; bottom, merge with NLS-GFP–β-Gal in green and tubulin in red.

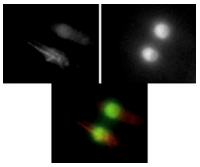

Video 3. **Efflux of the NLS-GFP–β-Gal fusion protein from the nuclei of *cut11.1* cells during mitosis.** *cut11.1* cells incorporating both integrated NLS-GFP–β-Gal and pRep81Cherry-tubulin plasmid were grown at 25°C and mounted for live imaging at 36°C. Time-lapse images were captured in both green and red channels every 4 min. The video is shown at 3 frames/s. Panels: top left, tubulin; top right, NLS-GFP–β-Gal; bottom, merge with NLS-GFP–β-Gal in green and tubulin in red.

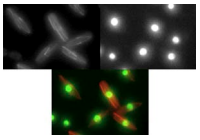

Video 4. **Efflux of the NLS-GFP–β-Gal fusion protein from the nuclei of *cut12.1* cells during mitosis.** *cut12.1* cells incorporating both integrated NLS-GFP–β-Gal and pRep81Cherry-tubulin plasmid were grown at 25°C and mounted for live imaging at 36°C. Time-lapse images were captured in both green and red channels every 4 min. The video is shown at 3 frames/s. Panels: top left, tubulin; top right, NLS-GFP–β-Gal; bottom, merge with NLS-GFP–β-Gal in green and tubulin in red.